Published in final edited form as:
J Proteome Res. 2009 July ; 8(7): 3727–3736. doi:10.1021/pr900294g.

Laser Trabeculoplasty Induces Changes in the Trabecular Meshwork Glycoproteome: A pilot study

Adriana Amelinckx[1,2], **Maria Castello**[1], **Esdras Arrieta-Quintero**[1,2], **Tinthu Lee**[1], **Nelson Salas**[2], **Eleut Hernandez**[1,2], **Richard K. Lee**[1], **Sanjoy K. Bhattacharya**[1], and **Jean-Marie A Parel**[1,2,3]

[1] Bascom Palmer Eye Institute, University of Miami Miller School of Medicine, Miami, Fl

[2] Ophthalmic Biophysics Center, University of Miami Miller School of Medicine, Miami, Fl

[3] Vision CRC, Sydney, Australia

Abstract

Laser trabeculoplasty (LT) is a commonly used modality of treatment for glaucoma. The mechanism by which LT lowers the intraocular pressure (IOP) is unknown. Using cat eyes, selective laser trabeculoplasty (SLT) with a Q-switched frequency doubled Nd:YAG laser was used to treat the trabecular meshwork (TM). Laser treated TM was then subjected to proteomic analysis for detection of molecular changes and histological analysis for the detection of structural and protein expression patterns. In addition, the protein glycosylation patterns of laser treated and non-treated TM was assessed and differentially glycosylated proteins were proteomically identified. SLT laser treatment to the TM resulted in elevated glycosylation levels compared to non-lasered TM. TM laser treatment also resulted in protein expression levels changes of several proteins. Elevated levels of biglycan, keratocan and prolargin were detected in laser treated TM compared to non-lasered controls. Further investigation is anticipated to provide insight into how glycosylation changes affect TM proteins and TM regulation of aqueous outflow in response to laser trabeculoplasty.

Keywords

Laser Trabeculoplasty; Proteoglycans; Trabecular Meshwork; Glaucoma

INTRODUCTION

Glaucoma is the one of the leading cause of irreversible visual impairment that affects over 70 million individuals world-wide [1]. Primary open angle glaucoma (POAG) and angle closure glaucoma (ACG) are expected to affect about ~80 million persons by the year 2020. Seventy-four percent of this population is predicted to have open angle glaucoma [2].

Laser trabeculoplasty (LT) is beneficial for certain patients with POAG [3]. LT is a non-invasive glaucoma treatment that has been employed as first line or adjunctive therapy, or in order to avoid or delay invasive incisional surgical procedures [4, 5]. Argon laser trabeculoplasty (ALT) produces a thermal burn on the surface of the TM that, over a period of 6–10 weeks, is associated

Address correspondence, proof and reprint request to: Jean-Marie A Parel, Ph.D. Ophthalmic Biophysics Center, Bascom Palmer Eye Institute, University of Miami, 1638 NW 10th Ave, Miami Fl 33136, Tel: 305-326-6369, Email: jmparel@med.miami.edu, Sanjoy K. Bhattacharya, M. Tech, Ph.D. Ocular Proteomics Laboratory, Bascom Palmer Eye Institute, University of Miami, 1638 NW 10th Ave, Miami Fl 33136, Tel: 305-482-4103, Email: Sbhattacharya@med.miami.edu.

The authors declare that they have no conflict of interest

with a reduction in intraocular pressure (IOP) [6]. The effect of ALT wanes over time and has been reported to have a 7 to 10% yearly failure rate [7]. Selective laser trabeculoplasty (SLT) is a relatively recently developed laser technique that has also been shown to effectively lower the IOP similar to ALT [8].

ALT is associated with significant tissue disruption. An understanding of the physiological pathway by which IOP is reduced by ALT is lacking, especially with regard to the cellular and molecular changes in the TM that need to occur over 1–2 months that cause IOP to be lowered. ALT has been used for nearly four decades [9], however, optimal operating parameters for ALT treatments have yet to be determined. Lack of knowledge regarding the cellular and molecular mechanism of action of ALT treatment on TM tissue inhibits our ability to design better and safer IOP lowering treatment parameters, predict the response to different kinds of laser energy, determine the duration of the laser effect (how long will IOP be decreased) and safety levels for repeated ALT treatment to the TM [10]. Even less is known about the molecular mechanisms by which SLT lower IOP through the TM.

TM cells possess a wide range of biochemical and structural properties, including the ability to synthesize glycosaminoglycans (GAGs), collagen, fibronectin, and other connective tissue elements [11]. Studies suggest shortening or tightening of the inner trabecular lamella, alteration in the TM cell population and extracellular matrix (ECM) synthesis can occur [10, 12]. However, the effect of SLT on TM tissue and its consequence (i.e. IOP lowering) is not evident by light or electron microscopy [13]. Therefore, dissection of the effect of SLT on the TM at the molecular level is necessary to elucidate modifications at the tissue and cellular level. SLT is believed to result in selective absorption of energy by pigmented TM cells, sparing adjacent cells and tissues from thermal damage compared to ALT. Morphologic studies demonstrate minimal tissue alteration following treatment with SLT [14]. Selective killing of cultured, pigmented TM cells has been demonstrated using a Q-switched, double-frequency, neodymium:yttrium–aluminum–garnet (Nd:YAG) laser [15]. SLT is believed to induce early cell division and these new cells have been proposed to migrate and re-populate the laser burn site [3]. Heat induced shrinkage of collagen within the trabecular beams secondary to laser treatment have been suggested versus mechanical re-shaping of the TM [16].

Glycosaminoglycans (GAGs) have been proposed to play a central role in maintaining the normal outflow resistance in human TM [17]. Increased expression of GAGs has been postulated to influence aqueous outflow resistance in the TM [17]. Previous reports have suggested laser treatment increases proteoglycan production by TM cells [3, 10].

This current work aims to determine protein changes in the TM following SLT and evaluates whether the presence of elevated glycoprotein in the TM occurs following laser treatment employing proteomic mass spectrometry and other techniques such as immunohistochemistry and enzyme linked immunosorbent assay (ELISA). Changes in the glycoproteome may lead to increased aqueous humor outflow and elucidate cellular and molecular mechanisms important for the treatment of glaucoma by lowering the IOP through changes in aqueous outflow.

MATERIALS AND METHODS

The cat eye model was selected as its anterior chamber dimension and tissue properties, as well as its optical access to laser trabeculoplasty, is similar to the human eye[13]. Two healthy domestic cats (*Felix domesticus*) with a total of four eyes between 6–8 months of age and weighing between 2.85–3.70 kg were used for these studies. Animal use procedures were approved by the University of Miami Institutional Animal Care and Use Committee and adhere to Association for Research in Vision and Ophthalmology (ARVO) guidelines regarding the

use of animals in vision research. Laser treatment and related experimental procedures were performed under general anesthesia with intramuscular injection of ketamine hydrochloride 20 mg/Kg (Ketaset III; Fort Dodge Animal Health, Fort Dodge, IA), acepromazine maleate 0.1 mg/kg (Boerhringer Ingelheim Vetmedica, Inc., St. Joseph, MO), and atropine sulfate 0.20 mg/kg (Phoenix Scientific, Inc. St. Joseph, MO). Eyes were divided into temporal and nasal halves. Cat # C03012 received 180 degree ALT (700 mW, 100μ spot size, 0.1 sec) in the temporal half of the left eye and SLT (1.32–1.91 mJ, 400μm spot size, 3ns) in the nasal half of the left eye and temporal half of right eye; the nasal half of the right eye was used as an internal non-lasered control. The second cat # C4001 received treatment only in the right eye: a 180 degree ALT the temporal half and nasal half of the right eye and the left eye served as a non-lasered control.

IOP measurements were performed before and after laser treatment with a Tonopen (Tono-Pen® XL, Reichert) and a handheld Perkins tonometer. The cats were assessed on post-operative days 1, 3, 7 and 14. The animals were euthanized two weeks after treatment and the enucleated eyes (4) were dissected under a surgical microscope (Topcon OMS 300), and fixed in 10% formalin or frozen for proteomic analysis. The cornea was excised circularly 2 mm parallel to the limbus, removed and then excised at the equator. The posterior segment including vitreous and lens were carefully removed and the remaining tissue was excised at the meridian into four equal parts. Each treated area of TM was cut into two sections: one was fresh frozen for proteomic analysis and the other was fixed for histological and immunohistochemical analysis.

Protein analysis

Dissected TM samples were placed into microfuge tubes and stored at −80 °C until further use. Proteins were extracted from dissected tissues using a base buffer (containing 125 mM Tris Cl buffer pH 7.0 and 100 mM NaCl) and a combination of detergents consisting of 0.1% Genapol C-100 (EMD Biosciences, CA), 1% Triton X-100 and 0.2% SDS in base buffer. Insoluble materials were removed by centrifugation (8000 × g for 5 min), and soluble proteins were quantified using the Bradford protein assay [18]. Proteins were fractioned by 4–20 % gradient sodium dodecyl sulfate polyacrylamide gel electrophoresis (SDS- PAGE), (Invitrogen Inc., Carlsbad, CA) and stained with SYPRO® Ruby (Molecular Probes, Invitrogen Inc., Carlsbad, CA) and/or Coomassie blue (Gel Code Blue; Pierce Biotechnology Inc, Rockford, IL) for detection of total protein. Protein bands were excised, de-stained, reduced with dithiotheritol (DTT), alkylated with iodoacetamide and subsequently processed for mass spectrometric analysis.

Staining for glycosylated proteins

Total glycosylated proteins were detected using the Gelcode Glycoprotein Staining Kit (Product # 24562; Pierce Biotechnology, Rockford, IL) following the manufacturer's instructions. This kit is designed for specific staining of glycoproteins directly within gels. A Pro Q Emerald 300 glycoprotein gel and blot stain kit (P21857; Molecular probes, Invitrogen Inc., Carsbald, CA) with suitable modification to stain gels was also used to stain identical gels along with the GelCode kit. The two kits differ with respect to their ability to stain proteins. Pro Q Emerald 300 Glycoprotein stain is 50-fold more sensitive than the GelCode staining kit. The GelCode staining kit uses periodic acid schiff base modification of carbohydrate groups that are stained with acidic fuschin dye to detect glycoproteins. Pro Q Emerald 300 utilizes a proprietary stain that reacts with periodate-oxidized carbohydrate groups to create bright fluorescent green signals on glycoproteins. Mass spectrometric compatibility for proteins stained with the GelCode kit remains to be established. Glycosylated protein bands stained by Pro Q Emerald 300 were excised, destained, reduced, alkylated (with iodoacetamide), and subjected to mass spectrometric analysis.

Mass Spectrometry

For protein identification, gel slices were excised and digested *in situ* with sequencing grade-modified trypsin (Promega Biosciences Inc, CA). Digestion mixtures were loaded onto pre-columns (360mm o.d, 100 mm i.d fused silica tube, Polymicron Technologies, Phoenix, AZ) packed with 3 cm irregular C18 (360 × 100). Once the columns were in-line, the peptides were gradient eluted with a gradient of 0–100%. All samples were analyzed using a LTQ mass spectrometer (Thermo Fischer, San Jose, CA). Electrospray was accomplished using a Advion Triversa Nanomate (Advion Biosystems Ithaca, NY) with a voltage of 1.7 kV and a flow rate of 250 nL/min. The mass spectrometer was operated in data-dependent mode with the top 5 most abundant ions in each spectrum being selected for sequential MS/MS experiments. The exclusion list was used (1 repeat, 180 sec return times) to increase the dynamic range. All MS/MS spectra were searched with SEQUEST (version 2.7), and Swiss-Prot, IPI and NCBI non-redundant databases. Search entries were performed on cats, mammalian and human databases since the cat database is not exhaustive. The protonated “MH” and “Monoisotopic” peptides were defined for the peak mass data input. For protonated “MH” peptides, SEQUEST Sp and Xcorr cutoff scores were 3.0 and 5.53. All spectra were visually inspected to determine correct database assignment. Database search results were tabulated and visually inspected using Scaffold visualization software (Proteome Software, Portland, OR).

Immunohistochemistry

Enucleated eye sections for fixation were processed by embedding in paraffin and sectioned into 10 μm slices using a Rotatory Microtome (Leitz 1512, Imeb Inc, Austria). Histological assessment of fixed TM tissue was performed using hematoxylin and eosin staining and imaged with an Olympus IX 50 microscope with a built-in imaging retina 1300 R fast 1394 digital camera. For immunohistochemistry, the specimens were initially stained with several antibodies, including rabbit polyclonal antibodies to cofilin-1, biglycan, (Abcam Inc., MA), mouse anti human keratocan (Invitrogen Inc., Carlsbad, CA) and mouse monoclonal anti-GAPDH (Chemicon Inc. Temecula, CA). Secondary antibodies were coupled with Alexa 594 (Invitrogen Inc., Carlsbad, CA). Secondary antibody only treated tissues served as a background staining controls. Immunofluorescence images were captured on a Leica TCS SP5 confocal microscope.

Enzyme linked immunosorbent assay (ELISA)

The amount of select proteins (GAPDH, biglycan and keratocan) were determined in TM samples of cats employing enzyme linked immunosorbent assay (ELISA). Protein samples were diluted 1:1000 in 1X phosphate buffered saline (PBS) and placed in microtiter plates (100 μL/well). Bovine serum albumin (BSA) was used as control. Microtiter wells were blocked by using 1% ovalbumin in 1 X PBS, 300 μL/well and the plate was incubated at 37°C. Primary antibody at 1:500 dilutions (in 1X PBS) was added and the microtiter plate was incubated at room temperature on a shaker for one hour. The plate was washed with 1X PBS three times and secondary antibody was then added (1:2000 dilution in 1X PBS), and incubated at room temperature for 1 hour. Supernatant was discarded and the plate was washed with 1X PBS three times. Finally 100 μL/well of 1mg/mL phosphate substrate in diethanolamine was added to each well. The plates were read at 450 nm in an ELISA plate reader (Titertek Multiskan Reader, Labsystems Multiskan, RC). The mean of measurements from three independent experiments was determined and the standard deviation was calculated.

RESULTS

The SLT treatment was uneventful and neither discomfort nor inflammation was observed in the cats during the 2 weeks of post-operative follow-up. Ocular hypertension was not observed

during the study period and the cornea, iris, lens, vitreous and retina remained normal and stable throughout the study.

Functional and histological integrity of anterior chamber tissues subjected to laser treatment

The mean pre-treatment IOP measured with a Perkins tonometer was 10.3 ± 2.6 mm Hg; the mean IOP post treatment was 5.3 ± 3.4 mm Hg. The mean IOP at post-operative day 14 was 8.8 ± 1.0 mm Hg. These values are similar to the findings of Stoiber, Fernandez et al, 2005[13]. Compared with the non-treated control eye, the IOP of the treated eyes was not significantly different at POD 14. Histological sections of anterior chamber tissue of non-treated and SLT treated cat eyes were performed to determine if any discernable histological changes occur in the TM due to SLT treatment. Two weeks post-treatment, the non-treated (Fig. 1A) and laser treated TM sections (Fig. 1B, C) displayed normal architecture of the sclera, TM, iris, ciliary body and cornea. Sections treated with selective laser trabeculoplasty (Fig. 1B) showed no modifications or inflammatory response in the TM.

Determination of protein changes in TM tissue subjected to laser trabeculoplasty treatment

TM protein extracted after laser trabeculoplasty treatment did not demonstrate any increase in viscosity or a significant decrease in protein recovery performed under identical condition for treated and non-treated ocular tissues (data not shown). Qualitatively extracted TM proteins were separated on one dimensional 4–15% SDS-PAGE (PHAST gel system; GE Healthcare Inc., CA). The gel was first subjected to glycosylation detection using the Gelcode Glycoprotein Staining Kit (Fig. 2A) followed by total protein staining with Coomassie blue, which revealed a lack of discernable difference between treated and non-treated TM protein lanes (Fig. 2B). Notably, a lack of elevated levels of high molecular weight proteins were observed in treated compared to control TM lanes. The most prominent glycosylated protein band was observed around molecular weight 36–40 kDa in treated samples compared to controls (Fig. 2A; indicated by the arrow). However, laser treated samples showed other glycosylated bands as well (Fig. 2A). The positive control glycosylated protein horseradish peroxidase was observed at a molecular weight of ~30 kDa, presumably a little lower than the reported size of 38 kDa. The LC MS/MS analysis of the overexpressed glycosylated band (Fig. 2A; indicated by arrow) identified five proteins. Three common glycosylated proteins (biglycan, keratocan and prolargin) were identified in the SLT treated lanes (Table 1).

In order to achieve better protein molecular weight separation and staining, a higher amount of total protein (20 μg) was electrophoresed in 1.5 mm 4–20% gradient mini-gels (Invitrogen Inc., Carlsbad, and Rockford, IL) and stained for protein glycosylation using the Gelcode Glycoprotein Staining Kit (Fig. 3A) with another glycoprotein stain, Pro Q Emerald 300 (Fig. 3B). The gel was also subsequently stained with Coomassie blue to assess total protein levels (Fig. 3C). Select gel bands that stained for Gelcode and Pro Q Emerald 300 were marked and equivalent bands in control and SLT lanes were marked (Fig. 3), excised, in-gel trypsin digested and subjected to LC MS/MS for protein identification (Table 2). Analyses revealed four proteoglycan/glycoproteins: fibromodulin, biglycan, keratocan, and prolargin in laser-treated tissues in multiple bands (Table 2; Fig. 3), although these proteins were also identified in controls but in fewer locations. This suggests that the identified proteoglycans are expressed in higher quantities and underwent aggregation as well as degradation compared to control TM tissue (Table 2). ADP ribosylation factor 1 was also identified in the SLT-treated tissue (Table 2) in this analysis, in contrast to our previous single band analysis (Fig. 2A; Table 1). This is likely due to the analysis of a single band in the previous analysis. A number of proteins identified in this analysis did not reveal glycosylated proteins despite staining by two different methods (Fig. 3) - this may be due to lack of knowledge of glycosylation for identified proteins or the presence of higher abundance proteins in the same bands which may mask glycosylated

proteins. A third possibility is that some of these stained bands have minimally glycosylated proteins that are resistant to trypsin digestion (Fig. 3; Table 2).

Determination of changes in the level of glycosylated proteins after laser trabeculoplasty treatment

Consistent identification of biglycan, keratocan and prolargin in the laser-treated TM samples (Table 1, 2) and the presence of prominent glycosylation staining protein bands (Fig. 2A) led us to test whether laser treated TM tissue had elevated levels of these proteins. Quantitative ELISA analysis of control and laser treated tissue with antibodies to biglycan and keratocan indeed showed the levels of these proteins are elevated in the SLT-treated tissue compared to non-treated controls. The level of GAPDH protein in ELISA was relatively lower than biglycan and keratocan in SLT-treated tissue derived proteins compared to non-treated controls (Fig. 4). In contrast to glycoproteins (biglycan and keratocan), the level of GAPDH remained similar in control and treated tissue indicating that expression levels of select LC MS/MS identified glycoproteins were elevated, as confirmed by ELISA analysis.

Localization of glycosylated proteins in the laser trabeculoplasty treated trabecular meshwork

A number of glycosylated proteins were found to be elevated in the laser treated eyes (Fig. 2, 3; Table 1, 2). The dissected TM tissue may be contaminated by surrounding sclera and cornea tissues. Therefore, immunohistochemical analyses were performed to demonstrate elevated levels of glycosylated proteins in SLT treated TM tissue. The tissue expression levels of proteoglycans biglycan (Fig. 5) and keratocan (Fig. 6) were found to be elevated in SLT-laser treated compared to control TM tissue. SLT laser treatment did not appear to affect keratocan levels (Fig. 5B, C). In contrast, the housekeeping protein GAPDH (Fig. 7) demonstrated very similar expression levels between the SLT treated and non-laser treated group, thereby corroborating the ELISA analysis (Fig. 4).

DISCUSSION

Light microscopic examination of TM tissue two weeks after SLT laser treatment did not show significant morphological change compared to non-lasered control TM tissue (Fig. 1). The decrease in intraocular pressure after laser trabeculoplasty is attributed to increased aqueous outflow through the anterior chamber aqueous outflow facility [19, 20]. This has been attributed to functional cell biological TM changes induced by laser trabeculoplasty treatment. Cellular and molecular changes in the laser treated TM must underlie the observed functional changes that are not obvious from light microscopy (Fig. 1). These findings are consistent with and corroborate previous reports which show a lack of morphological changes at the microscopic or ultra-structural level after LT, with the exception of slight alterations in pigment containing cells [13, 21].

Laser treatment has been reported to result in increased metabolic activity [6, 16] and cell division in the TM cells re-populating the laser burn site [3]. TM cells can synthesize glycosaminoglycans (GAGs) locally [11] and laser treatment has been reported to induce increased expression of GAGs by TM cells [6, 10]. Recent studies suggest biophysical cues play a profound role in TM cell expansion and remodeling [22]. Whether increased expression of GAGs due to laser treatment modulates the extracellular matrix (ECM) environment and enable TM cells to respond to biophysical cues with remodeling, which in turn result in increased outflow facility and lower IOP, remains to be determined. The trabecular cell surfaces and the inter-trabecular spaces are lined with mucinous GAGs [23]. Three distinct types of sulfated proteoglycans are found in human trabecular tissue: chondroitin sulfate, dermatan sulfate and heparan sulfate [24]. These proteoglycans are important contributors to aqueous outflow resistance in the

juxtacanalicular connective tissue [3, 25]. Decorin, biglycan, versican and perlecan core proteins have been identified by immunoblot analysis of trabecular cell extracts [26]. GAGs are believed to regulate TM fluid outflow by forming viscoelastic gel-like solutions [27] and likely play a role in fluid dynamics by modulating the TM extracellular matrix [28]. The accumulation of dermatan in the sclera leads to an increase in flow resistance, and can produce uveal effusion syndrome [29]. The loss of chondroitin sulfate (CS-PG) and heparan sulfate (HS-PG) proteoglycans has been attributed to failure of tissue fluid homeostasis in severe lung edema. Exposure to heparinase that cleave PGs results in loss of fluid homeostasis in the lung tissue, thereby suggesting a stabilization of PGs of the matrix architecture that ensures adequate mechanical responses to fluid load [30]. PGs have also found to play a prominent role in fluid flow in the kidneys [31] and have been implicated in a number of kidney diseases [32, 33].

Alterations in TM glycosaminoglycan levels correlate with increased resistance to aqueous drainage in primary open angle glaucoma [34]. Patients with glaucoma have been shown to have substantially reduced levels of hyaluronic acid in the entire TM as well as in the juxtacanalicular tissue [35]. Significant changes in the qualitative and quantitative composition of GAGs (decreased sulfated GAGs and increased collagen-bound PGs) was observed in the TM of in primary juvenile glaucoma [36]. Topical application of decorin, a PG have been shown to improve outcome of glaucoma filtration surgery in an animal model [37].

Diminished juxtacanalicular ECM turnover is associated with reduction in the aqueous humor outflow associated with glaucoma. PGs are important for maintaining ECM turn-over. Several PGs have been shown to modulate TM ECM. For example, heparin interferes with specific interactions between cells and ECM proteins in the TM that regulate outflow facility [38] and up-regulated versican has been found in human TM cells treated with TGF-β [39]. In the ECM, collagen bound PGs show differences between normal and glaucomatous eyes [40].

Our analyses revealed elevated presence of biglycan, prolargin, keratocan, and cofilin-1, an actin-binding factor required for the organization of actin filaments, in the TM (Table 1, 2 and Fig. 4). These proteins were upregulated in laser treated eyes compared non-treated controls. We have used SLT treatment and also ALT treatment (data not shown) on cat eyes, however, further comparative studies on a greater number of tissues and quantitative proteomic assessment such as ITRAQ quantitation[41] is necessary to find out comparative differences between SLT and ALT treated tissue. These studies are currently under progress. The changes in ALT treated tissues were less pronounced and these analysis will be performed with a greater number of eyes to effectively capture changes in the tissues due to ALT treatment.

Biglycan is a small leucine-rich repeat proteoglycans (SLRPS) consisting of a protein core containing leucine-rich repeat regions and two GAGs chains associated with either chondroitin sulfate (CS) or dermatan sulfate (DS). Biglycan interacts with collagen VI and complement component C1q [42, 43]. Biglycan has been implicated in the regulation of collagen fibrillogenesis and plays a role in aqueous fluid dynamics and sclera development and repair. Keratocan and fibromodulin are proteins with a keratan sulfate (KS) core that is N-linked to specific asparagines amino acids via N-acetylglucosamine [44] and are members of the proline/arginine-rich end leucine-rich repeat protein (PRELP) family. The other members of this family are lumican, mimecan, osteoadherin and aggrecan.

Keratocan is an important sulfate PG controlling the organization of collagen fibrils in the cornea. Keratocan contributes to corneal transparency and plays a role in regulating neutrophil accumulation [45]. PRELPs have been implicated in Hutchinson-Gilford progeria disease, which is caused by a lack of collagen binding in basement membranes[46]. PRELP have been suggested to play a critical role in regulating the biomechanical properties of sclera ECM [47]. Abnormal

upregulation of expression of another proteoglycan, Aggregan, has also been found in Hutchinson-Gilford Progeria Syndrome dermal fibroblasts[48].

Prolargin, whose precursor is a member of the PRELP protein family, is a small leucine-rich proteoglycan. This protein serves as a molecular anchor to basement membranes in connective tissue. Prolargin is found in cartilage matrix peptides together with biglycan and plays a role in cartilage degradation and chondrocyte signaling [49]. Biglycan and prolargin are present in the intima of arteries and have been implicated in the pathogenesis of atherosclerosis [50].

Cofilin is a member of the ADF/cofilin family and is an intracellular actin-modulating protein that binds and depolymerizes filamentous F-actin and inhibits the polymerization of monomeric G-actin [51]. Cofilin is involved in the translocation of actin-cofilin complexes from the cytoplasm to the nucleus. Laser trabeculoplasty results in an increase in stromelysin [52]. It is plausible that increased levels of stomelysin, which degrades trabecular glycoproteins, could improve aqueous humor outflow [4]. Many PGs were found to be expressed at higher as well as lower molecular weight regions in the SDS-PAGE (Fig. 2, 3, Table 1, 2) suggesting these proteins undergo cross-linking as well as proteolytic degradation.

In summary, we observed increased expression of glycoproteins in the proteome of TM sections treated with SLT compared to non-lasered control TM. A greater understanding of the role of glycosylation of TM proteins induced by laser trabeculoplasty may offer insight into new modalities for decreasing outflow resistance by the TM. These insights will have significant importance for the development of new medications to treat glaucoma by lowering the intraocular pressure.

Acknowledgments

Supported in part by: Florida Lions Eye Bank; CromaPharma GmbH, Vienna (JMP), Austria; NIH grants EY15266, EY016775 and P30EY14801; a Career Award (SKB) and an unrestricted grant from Research to Prevent Blindness and the Henri and Flore Lesieur Foundation (JMP).

References

1. Quigley HA. Number of people with glaucoma worldwide. Br J Ophthalmol 1996;80:389–93. [PubMed: 8695555]
2. Quigley HA, Broman AT. The number of people with glaucoma worldwide in 2010 and 2020. Br J Ophthalmol 2006;90:262–267. [PubMed: 16488940]
3. Acott TS, Samples JR, Bradley JM, Bacon DR, Bylsma SS, Van Buskirk EM. Trabecular repopulation by anterior trabecular meshwork cells after laser trabeculoplasty. Am J Ophthalmol 1989;107:1–6. [PubMed: 2912110]
4. Rolim CP, Wormald AR. Laser Trabeculoplasty for open angle glaucoma (Review) The Cochrane Collaboration. 2008
5. Mahar PS, Jamali KK. Argon laser trabeculoplasty as primary therapy in open angle glaucoma. J Coll Physicians Surg Pak 2008;18:102–104. [PubMed: 18454896]
6. Alexander RG I, Church W. The effect of argon laser trabeculoplasty upon the normal human trabecular meshwork. Graffe's Arch Clin Exp Ophthalmology 1989;227:72–77.
7. Morrison, JP.; Glaucoma, I. Science and Practice. Vol. I. Thieme Medical Publishers; New York: 2003.
8. Kramer TR, Noecker RJ. Comparison of the morphologic changes after selective laser trabeculoplasty and argon laser trabeculoplasty in human eye bank eyes. Ophthalmology 2001;108:773–779. [PubMed: 11297496]
9. Ritch, RS.; Krupin, MBT. Glaucoma Therapy. Vol. 2. Vol. III. St. Louis; 1989. The Glaucoma; p. 1575-1590.
10. Van Buskirk EM. Argon Laser Trabeculoplasty. Ophthalmology 1984;91:1005–1009. [PubMed: 6493712]

11. Polansky JR, Wood IS, Maglio MT, Alvarado JA. Trabecular meshwork cell culture in glaucoma research: evaluation of biological activity and structural properties of human trabecular cells in vitro. Ophthalmology 1984;91:580–595. [PubMed: 6540429]
12. Melamed S. Trabecular repopulation by anterior trabecular meshwork cells after laser trabeculoplasty. Am J Ophthalmol 1989;108:209–210. [PubMed: 2502925]
13. Stoiber J, Fernandez V, Lamar PD, Decker SJ, Dubovy S, Hitzl W, Salas N, Fantes F, Parel JM. Trabecular meshwork alteration and intraocular pressure change following pulsed near-infrared laser trabeculoplasty in cats. Ophthalmic Surg Lasers Imaging 2005;36:471–481. [PubMed: 16358427]
14. Barkana Y, Belkin M. Selective laser trabeculoplasty. Surv Ophthalmol 2007;52:634–654. [PubMed: 18029271]
15. Latina MA, Park C. Selective targeting of trabecular meshwork cells: in vitro studies of pulsed and CW laser interactions. Exp Eye Res 1995;60:359–371. [PubMed: 7789416]
16. Bylsma SS, Samples JR, Acott TS, Van Buskirk EM. Trabecular cell division after argon laser trabeculoplasty. Arch Ophthalmol 1988;106:544–547. [PubMed: 3355425]
17. Cavallotti C, Feher J, Pescosolido N, Sagnelli P. Glycosaminoglycans in human trabecular meshwork: age-related changes. Ophthalmic Res 2004;36:211–217. [PubMed: 15292659]
18. Bradford MM. A rapid and sensitive method for the quantitation of microgram quantities of protein utilizing the principle of protein-dye binding. Anal Biochem 1976;72:248–254. [PubMed: 942051]
19. Yablonski ME, Cook DJ, Gray J. A fluorophotometric study of the effect of argon laser trabeculoplasty on aqueous humor dynamics. Am J Ophthalmol 1985;99:579–582. [PubMed: 4003496]
20. Brubaker RF, Liesegang TJ. Effect of trabecular photocoagulation on the aqueous humor dynamics of the human eye. Am J Ophthalmol 1983;96:139–147. [PubMed: 6683934]
21. Starita RJ, Rodrigues MM, Fellman RL, Spaeth GL. Histopathologic verification of position of laser burns in argon laser trabeculoplasty. Ophthalmic Surg 1984;15:854–858. [PubMed: 6504504]
22. Gasiorowski JZ, Russell P. Biological properties of trabecular meshwork cells. Exp Eye Res 2009;88:671–675. [PubMed: 18789927]
23. Zimmerman LE. Demonstration of hyaluronidase-sensitive acid mucopolysaccharide in trabecula and iris in routine paraffin sections of adult human eyes; a preliminary report. Am J Ophthalmol 1957;44:1–4. [PubMed: 13435316]
24. Tawara A, Varner HH, Hollyfield JG. Distribution and characterization of sulfated proteoglycans in the human trabecular tissue. Invest Ophthalmol Vis Sci 1989;30:2215–2231. [PubMed: 2793361]
25. Acott TS, Kelley MJ. Extracellular matrix in the trabecular meshwork. Exp Eye Res 2008;86:543–561. [PubMed: 18313051]
26. Wirtz MK, Bradley JM, Xu H, Domreis J, Nobis CA, Truesdale AT, Samples JR, Van Buskirk EM, Acott TS. Proteoglycan expression by human trabecular meshworks. Curr Eye Res 1997;16:412–421. [PubMed: 9154378]
27. Knepper PA, McLone DG. Glycosaminoglycans and outflow pathways of the eye and brain. Pediatr Neurosci 1985;12:240–251. [PubMed: 3916537]
28. Francois J. The importance of the mucopolysaccharides in intraocular pressure regulation. Invest Ophthalmol 1975;14:173–176. [PubMed: 123231]
29. Forrester JV, Lee WR, Kerr PR, Dua HS. The uveal effusion syndrome and trans-scleral flow. Eye 1990;4(Pt 2):354–365. [PubMed: 2379646]
30. Negrini Daniela PA. Moriondo Andrea., the role of proteoglycans in pulmonary edema development. Intensive Care med 2008;34:610–618. [PubMed: 18264693]
31. Pyke C, Kristensen P, Ostergaard PB, Oturai PS, Romer J. Proteoglycan expression in the normal rat kidney. Nephron 1997;77:461–470. [PubMed: 9434070]
32. Bjornson Granqvist A, Ebefors K, Saleem MA, Mathieson PW, Haraldsson B, Nystrom JS. Podocyte proteoglycan synthesis is involved in the development of nephrotic syndrome. Am J Physiol Renal Physiol 2006;291:F722–F730. [PubMed: 16622173]
33. Kastner S, Thomas GJ, Jenkins RH, Davies M, Steadman R. Hyaluronan induces the selective accumulation of matrix- and cell-associated proteoglycans by mesangial cells. Am J Pathol 2007;171:1811–1821. [PubMed: 17974600]

34. Oh DJ, Martin JL, Williams AJ, Russell P, Birk DE, Rhee DJ. Effect of latanoprost on the expression of matrix metalloproteinases and their tissue inhibitors in human trabecular meshwork cells. Invest Ophthalmol Vis Sci 2006;47:3887–3895. [PubMed: 16936101]
35. McCarty MF. Primary open-angle glaucoma may be a hyaluronic acid deficiency disease: potential for glucosamine in prevention and therapy. Medical Hypotheses 1998;51:483–484. [PubMed: 10052867]
36. Kuleshova ON, Zaidman AM, Korel AV. Glycosaminoglycans of the trabecular meshwork of the eye in primary juvenile glaucoma. Bull Exp Biol Med 2007;143:381–384. [PubMed: 18225769]
37. Grisanti S, Szurman P, Warga M, Kaczmarek R, Ziemssen F, Tatar O, Bartz-Schmidt KU. Decorin modulates wound healing in experimental glaucoma filtration surgery: a pilot study. Invest Ophthalmol Vis Sci 2005;46:191–196. [PubMed: 15623773]
38. Santas AJ, Bahler C, Peterson JA, Filla MS, Kaufman PL, Tamm ER, Johnson DH, Peters DM. Effect of heparin II domain of fibronectin on aqueous outflow in cultured anterior segments of human eyes. Invest Ophthalmol Vis Sci 2003;44:4796–4804. [PubMed: 14578401]
39. Zhao XRP. Versican splice variants in human trabecular meshwork and ciliary muscle. Molecular Vision 2005;11:603–608. [PubMed: 16110303]
40. Lutjen-Drecoll E, Futa R, Rohen JW. Ultrahistochemical studies on tangential sections of the trabecular meshwork in normal and glaucomatous eyes. Invest Ophthalmol Vis Sci 1981;21:563–573. [PubMed: 7287346]
41. Ross PL, Huang YN, Marchese JN, Williamson B, Parker K, Hattan S, Khainovski N, Pillai S, Dey S, Daniels S, Purkayastha S, Juhasz P, Martin S, Bartlet-Jones M, He F, Jacobson A, Pappin DJ. Multiplexed protein quantitation in Saccharomyces cerevisiae using amine-reactive isobaric tagging reagents. Mol Cell Proteomics 2004;3:1154–1169. [PubMed: 15385600]
42. Krumdieck R, Hook M, Rosenberg LC, Volanakis JE. The proteoglycan decorin binds C1q and inhibits the activity of the C1 complex. J Immunol 1992;149:3695–3701. [PubMed: 1431141]
43. Hocking AM, Strugnell RA, Ramamurthy P, McQuillan DJ. Eukaryotic expression of recombinant biglycan. Post-translational processing and the importance of secondary structure for biological activity. J Biol Chem 1996;271:19571–19577. [PubMed: 8702651]
44. Funderburgh JL. Keratan sulfate: structure, biosynthesis, and function. Glycobiology 2000;10:951–958. [PubMed: 11030741]
45. Carlson EC, Lin M, Liu CY, Kao WW, Perez VL, Pearlman E. Keratocan and lumican regulate neutrophil infiltration and corneal clarity in lipopolysaccharide-induced keratitis by direct interaction with CXCL1. J Biol Chem 2007;282:35502–35509. [PubMed: 17911102]
46. Lewis M. PRELP, collagen, and a theory of Hutchinson-Gilford progeria. Ageing Res Rev 2003;2:95–105. [PubMed: 12437997]
47. Johnson JM, Young TL, Rada JA. Small leucine rich repeat proteoglycans (SLRPs) in the human sclera: identification of abundant levels of PRELP. Mol Vis 2006;12:1057–1066. [PubMed: 17093390]
48. Lemire JM, Patis C, Gordon LB, Sandy JD, Toole BP, Weiss AS. Aggrecan expression is substantially and abnormally upregulated in Hutchinson-Gilford Progeria Syndrome dermal fibroblasts. Mech Ageing Dev 2006;127:660–669. [PubMed: 16650460]
49. Zhen EY, Brittain IJ, Laska DA, Mitchell PG, Sumer EU, Karsdal MA, Duffin KL. Characterization of metalloprotease cleavage products of human articular cartilage. Arthritis Rheum 2008;58:2420–2431. [PubMed: 18668564]
50. Glowniak JV, Wilson RA, Joyce ME, Turner FE. Evaluation of metaiodobenzylguanidine heart and lung extraction fraction by first-pass analysis in pigs. J Nucl Med 1992;33:716–723. [PubMed: 1569481]
51. Bamburg JR. Proteins of the ADF/cofilin family: essential regulators of actin dynamics. Annu Rev Cell Dev Biol 1999;15:185–230. [PubMed: 10611961]
52. Parshley DE, Bradley JM, Fisk A, Hadaegh A, Samples JR, Van Buskirk EM, Acott TS. Laser trabeculoplasty induces stromelysin expression by trabecular juxtacanalicular cells. Invest Ophthalmol Vis Sci 1996;37:795–804. [PubMed: 8603864]

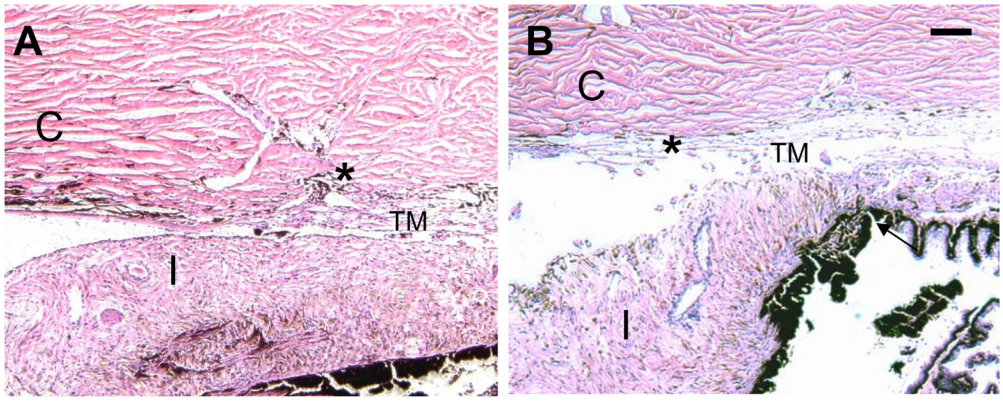

Figure 1.

Hematoxlyn-eosin stained anterior chamber section of cat eyes. **A**. Control (non-laser treated) eyes displaying histological structure of the anterior segment. **B**. A representative anterior eye section that underwent selective laser trabeculoplasty (SLT). No significant structural changes were found between control and treated trabecular meshwork. The location of the Cornea (C), Iris (I) and Trabecular meshwork (TM) are as indicated. (*) identifies Schlemm's canal (SC), Bar = 100 μm.

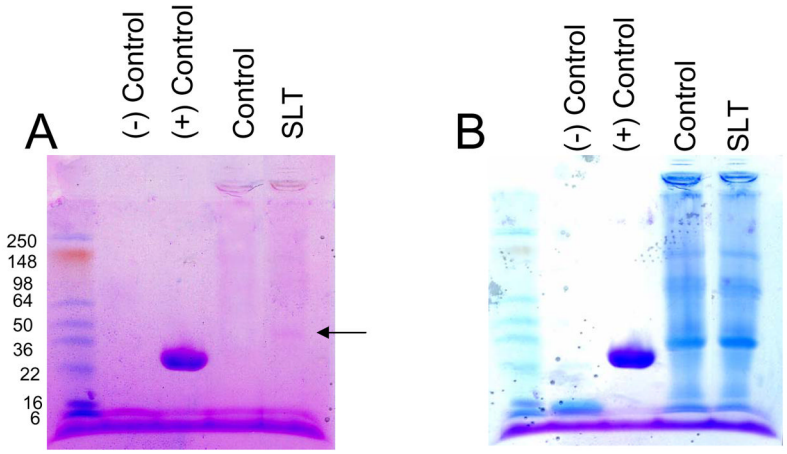

Figure 2.

Analysis of trabecular meshwork glycoproteome changes after laser trabeculoplasty. Control and laser treated cat TM tissue (10 μg), as indicated was extracted and fractionated over 4–15% SDS-PAGE (PHAST gel system, GE Healthcare Inc., CA) and stained for glycosylated or total protein. **A.** Staining for the glycoproteome using a glycoprotein staining kit (24562; Pierce Biotechnology Inc., Rockford, IL), prominent glycosylated protein band indicated by arrow was excised and subjected to LS MS/MS analyses. Negative and positive controls are soybean trypsin inhibitor and horse radish peroxidase, respectively. Molecular weights of proteins are as indicated. **B.** The same gel was subsequently subjected to total protein staining with Coommassie blue (Gel code blue).

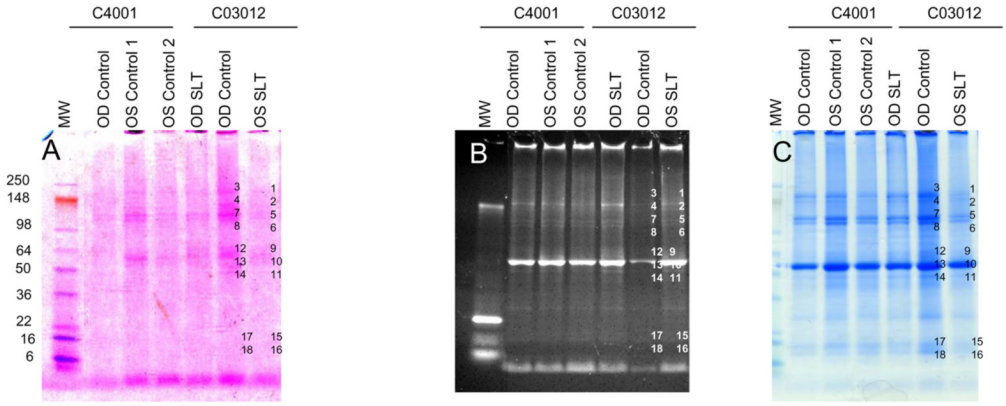

Figure 3.

Fractionation of protein extracts (20μg) from trabecular meshwork of cats C04-001 and C03-012 subjected to laser trabeculoplasty (SLT) as indicated on a 4–20% SDS-PAGE (1.5 mm minigel, Invitrogen Inc, Carlsbad, CA). **A.** Gel fractionated proteins were stained with Gelcode Glycoprotein Staining Kit (Pierce Biotechnology, Rockford, IL). **B**. Proteins were stained with Pro Q Emerald 300 glycoprotein gel and Blot stain kit (Molecular Probes) and, **C**. Proteins stained with Coomassie (Gel code blue; Pierce Biotechnology) to detect total proteins.

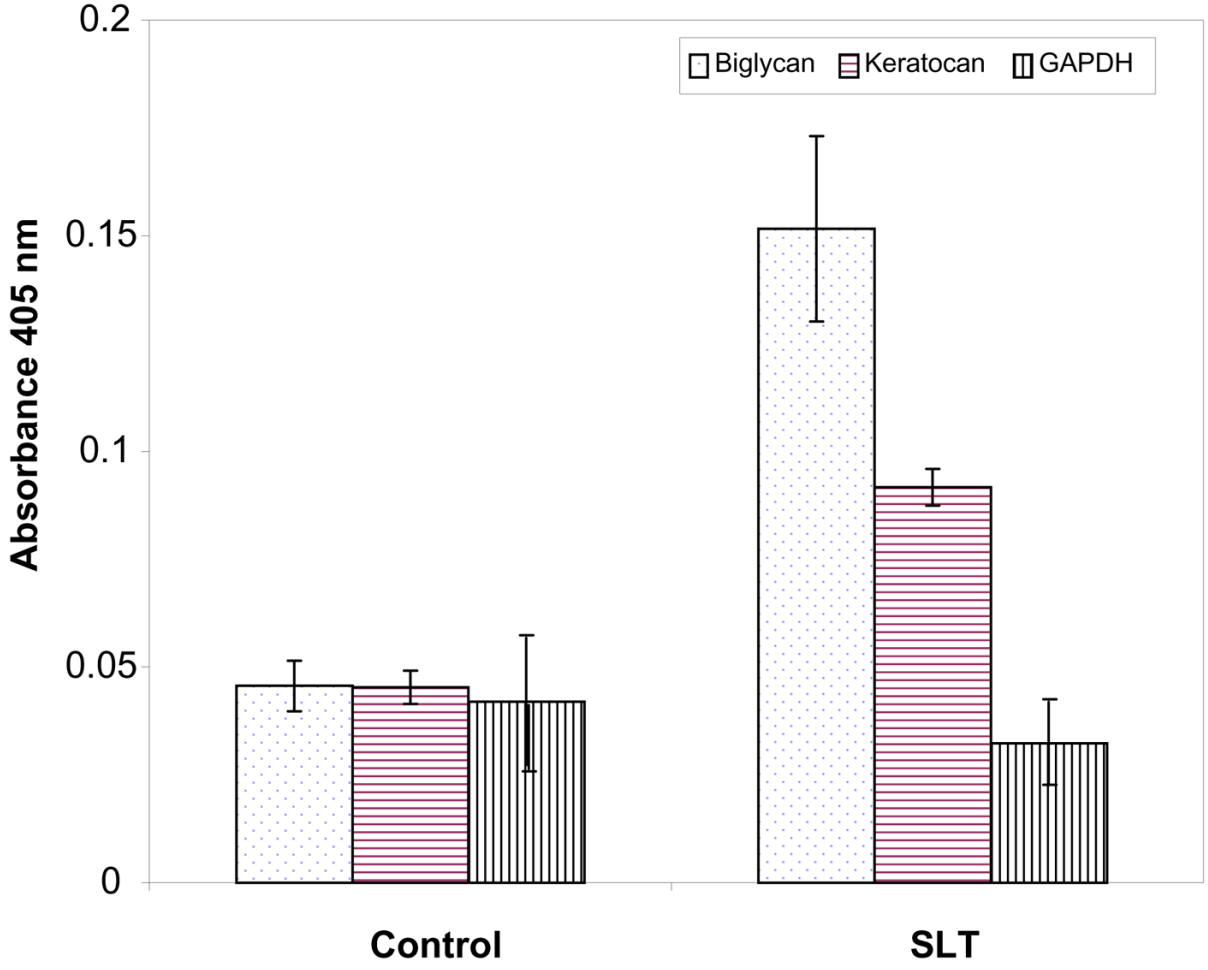

Figure 4.
Quantitative determination of biglycan, keratocan and glyceraldehyde-3-phosphate dehydrogenase (GAPDH), represented by symbols as indicated in control and laser treated trabecular meshwork. Relative levels of biglycan and keratocan are higher in SLT than in control TM. Standard deviations from three different experiments are presented.

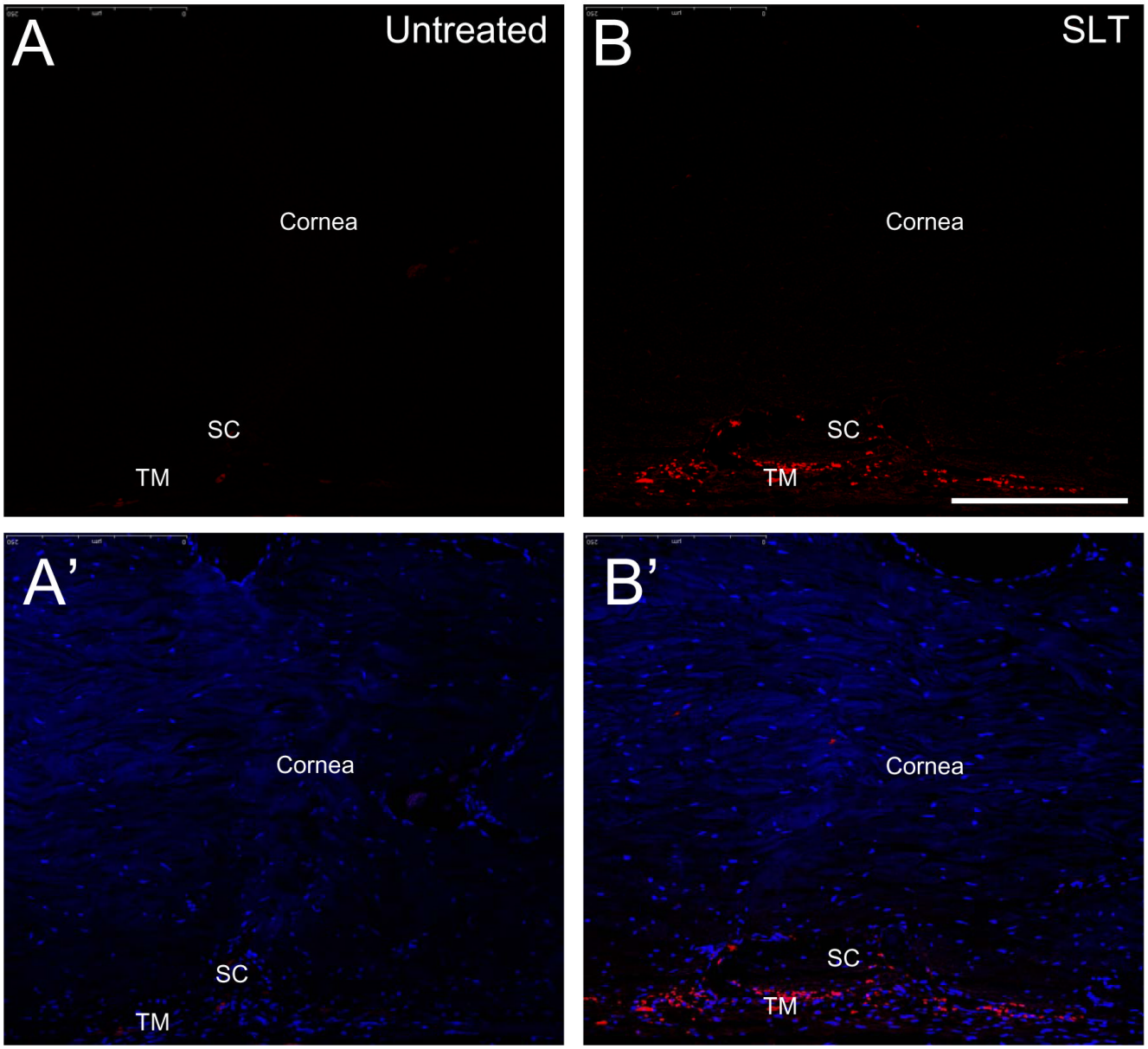

Figure 5.

Immunohistochemical detection of biglycan in the cat trabecular meshwork. Anterior eye sections (10 μm) were subjected to staining with rabbit polyclonal antibody to biglycan (Abcam Inc). **A.**, **A′**. Untreated eye, **B., B.′** selective laser trabeculoplasty treated eyes subjected to anti-biglycan and DAPI staining, respectively. SC and TM indicate Schlemm's canal and trabecular meshwork, respectively. Bar= 50 μm.

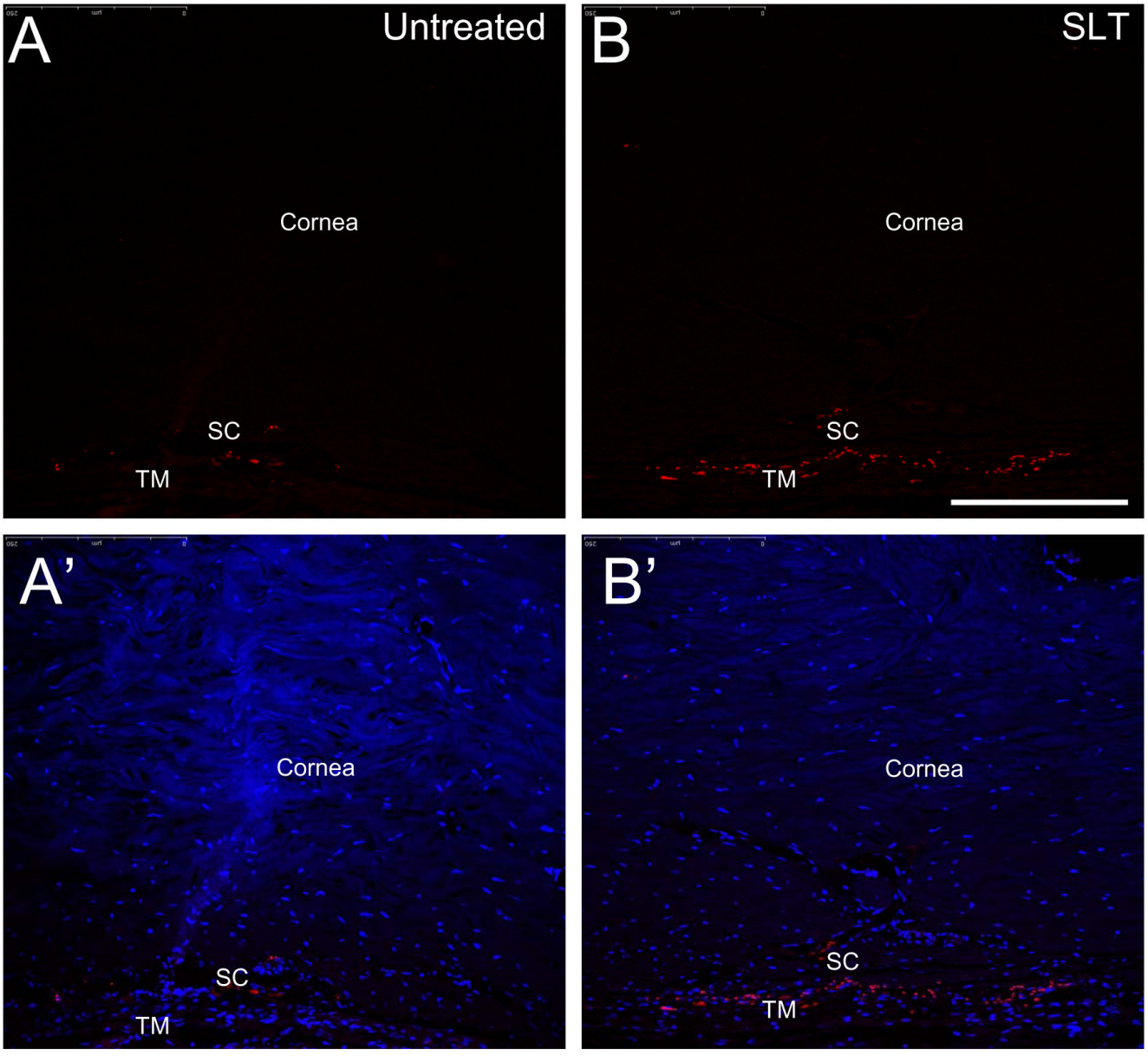

Figure 6.

Immunohistochemical detection of keratocan in the cat trabecular meshwork. The anterior eye sections (10 μm) were stained with mouse polyclonal antibody to human keratocan (Invitrogen Inc). **A.**, **A′**. Untreated eye, **B., B.′** selective laser trabeculoplasty treated eyes subjected to anti-keratocan and DAPI staining, respectively. SC and TM indicate Schlemm's canal and trabecular meshwork respectively. Bar= 50 μm.

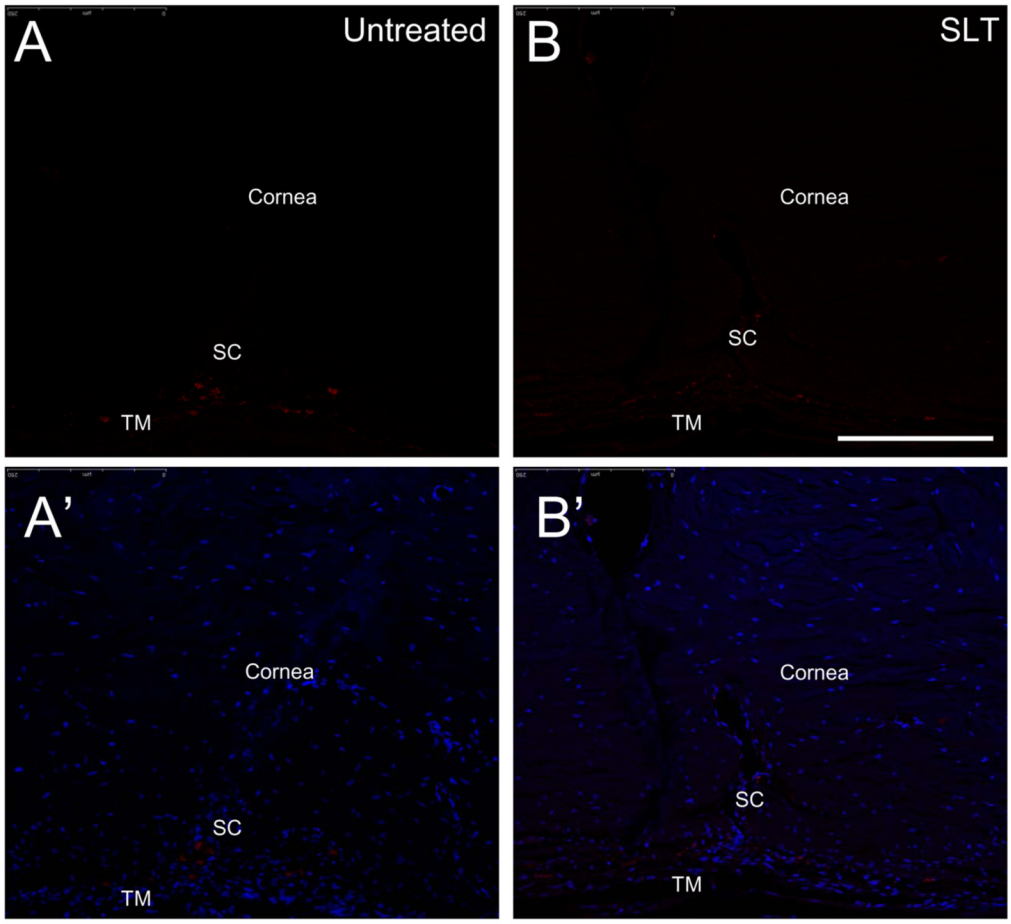

Figure 7.

Immunohistochemical detection of glyceraldehydes-3-dehydrogenase (GAPDH) in the cat trabecular meshwork. The anterior eye sections (10 μm) were subjected to staining with monoclonal antibody to cat GAPDH (Chemicon Inc., Temecula, CA). **A.**, **A′**. Untreated eye, **B., B.′** selective laser trabeculoplasty treated eyes subjected to anti-GAPDH and DAPI staining, respectively. SC and TM indicate Schlemm's canal and trabecular meshwork respectively. Bar= 50 μm.

Table 1

Proteins identified in the glycosylated band in laser treated trabecular meshwork

Accession Number	Protein Name	MW (KDa)	Peptide Matches	Sequence coverage (%)
IPI00010790	Biglycan	42	5	28
IPI00334627	Annexin A2 isoform 1*	39	2	9
IPI00013049	Keratocan	40	2	8
IPI00020987	Prolargin	43	2	8

Accession numbers are from IPI database.

* Identified in all laser treated and in the control at a band in equivalent position indicated by the arrow in Figure 2. The numbers in parenthesis indicates number of peptides identified in SLT.

Table 2

Identification of proteins in cat trabecular meshwork

Accession number*	Protein name	MW (kDa)	Peptide Matches	Sequence coverage (%)	Band number (control)	Band number (SLT)
IPI00302944	Isoform 4 of Collagen alpha-1 (XII) chain	324	7	3	3, 4	1, 2
BAA87071	ATP-binding cassette**	128	5	17	4, 7, 8	1, 2, 5
NP_001002011	Lamin A isoform A	74	2	10	8, 12, 13	5, 6, 9
IPI00003865	Isoform 1 of Heat shock cognate 71 kDa protein	70	3	3	7, 12, 13	5, 6, 9, 10
P49064	Albumin**	68	8	60	12, 13	5, 6, 9, 10
IPI00220327	Keratin, type II cytoskeletal 1	66	2	17	12, 13	
IPI00021304	Keratin, type II cytoskeletal 2 epidermal	65	3	21	12, 13, 14	
IPI00019359	Keratin, type I cytoskeletal 9	62	3	18	12, 13, 14	9
BAF82934	Keratin 6A	60	3	13	13, 14	9, 10
IPI00418471	Vimentin	53	5	30	13, 14	10, 11
2JIZD	F-ATPase (chain-D)	51	3	18	13, 14	10, 11
BAF82172	Tubulin alpha 1a	50	2	6	14, 17, 18	11, 15, 16
IPI00166768	Tubulin alpha 1c	49	5	9	14, 17, 18	11, 15, 16
ABD77244	Mitochondrial ATP synthase**	45	2	15	14, 17	5, 11, 15
IPI00000860	**Fibromodulin**	43	5	20	14, 18	6, 9, 10, 11, 15
IPI00020987	**Prolargin**	43	5	31	14	9, 10, 11, 15
IPI00215914	ADP-ribosylation factor 1	21	3	25		15, 16
IPI00021439	Actin, cytoplasmic 1	41	2	12	14, 17, 18	11, 15, 16
IPI00010790	**Biglycan**	41	5	20	17	9, 10, 11
BAF84626	Actin gamma 1	41	4	22	14, 17, 18	11, 15, 16
IPI00418169	Annexin A2 isoform 1	40	5	17	7, 14, 17	10, 11, 15, 16
IPI00013049	**Keratocan**	40	3	25	4, 14	10, 11, 15
BAA32229	IgG1 heavy chain**	36	2	17	14, 17, 18	11, 15, 16
BAB77244	Actin (β-actin)**	32	2	15	14, 17, 18	11, 15, 16
1CWCA	Cyclosporin (chain-A)	17	14	14		15, 16
IPI00419585	Peptidyl-prolyl cis-trans isomerase A	17	2	14	17	15, 16
IPI00654755	Globin (β-globin)	15	3	14	3, 17, 18	15, 16

J Proteome Res. Author manuscript; available in PMC 2010 July 1.

Accession number*	Protein name	MW (kDa)	Peptide Matches	Sequence coverage (%)	Band number (control)	Band number (SLT)
P07405	Hemoglobin subunit alpha**	15	2	36	4, 17, 18	2, 15, 16
P07412	Hemoglobin subunit beta-A/B**	15	2	32	17, 18	15, 16
AAH10564	Histone cluster 2, H2aa1	14	5	27	17, 18	15, 16
CAJ28937	Haptoglobin**	13	3	23	17, 18	15, 16
IPI00012011	Cofilin-1	18	5	30	17	15, 16
IPI00081836	Histone H2A type 1-H	13	11	27	17, 18	15, 16
AA114197	H4 protein	11	4	31	17, 18	15, 16
IPI00453473	Histone H4	11	3	31	17, 18	15, 16

* IPI database accession numbers begin with a prefix IPI, the NCBI protein database entries are in italics and all other accession numbers (six character beginning with letter P) are from Swiss-Prot database.

** The entries pertain to cats (*Felis catus*).